

Excited states in ^{69}Ga

P. Bakoyeorgos and T. Paradellis

*Tandem Accelerator Laboratory, Nuclear Research Center Demokritos,
Aghia Paraskevi, Athens, Greece*

P. A. Assimakopoulos

The University of Ioannina, Ioannina, Greece

(Received 22 February 1982)

Excited states in ^{69}Ga have been studied by the $^{64}\text{Ni} + ^7\text{Li}$ reaction at 18 MeV bombarding energy. Gamma-gamma coincidences, angular distribution, and centroid shift measurements are used to determine spin and mean lives in this nucleus. In addition to a positive parity band extending up to $J^\pi = 17/2^+$, a negative parity band built on a $9/2^-$ level has been also identified.

NUCLEAR REACTIONS $^{64}\text{Ni}(^7\text{Li}, 2n)^{69}\text{Ga}$ $E = 14 - 18$ MeV. Measured γ - γ , $I_\gamma(\theta)$, $E_\gamma(\theta)$, Doppler attenuation centroid shift. ^{69}Ga deduced J^π , δ , τ . Enriched target Ge(Li) detectors.

I. INTRODUCTION

Information concerning the low spin states in ^{69}Ga is available today from the study of the decay of the radioactive ^{69}Ga nucleus,¹ inelastic neutron scattering,² resonance fluorescence,³ and gamma-gamma directional correlation⁴ experiments. A review of all available information up to 1975 is given by Auble.⁵ More recently, experimental results obtained from the $(p, p\gamma)$, $(n, n\gamma)$, and (p, γ) reactions have also been published,⁶⁻⁸ enriching the available experimental information on the low spin levels of this nucleus.

Concerning high spin states in ^{69}Ga , the only data available is from the work of Harms-Rindgall *et al.*⁹ who use the $(\alpha, p\gamma)$ reaction. In the present work, the high spin states in ^{69}Ga are studied by the $^{64}\text{Ni} + ^7\text{Li}$ reaction which yields new valuable information on the structure of the high spin states in ^{69}Ga .

II. EXPERIMENTAL

A. Targets and reactions

Self-supported nickel foils of 4 mg/cm² thickness, enriched to 99% in ^{64}Ni have been used in the present experiments. The ^7Li beam was provided by the T11/25 tandem Van de Graaff accelerator of the Nuclear Research Center (NRC) "Demokritos." Bombarding energies varied between 14 and 18

MeV, depending upon the particular problem studied, while typical currents used were of the order of 10 nA to avoid large counting rates.

Gamma rays resulting from the bombardment were observed with the aid of two Ge(Li) detectors of 18% and 13% efficiency and a resolution of 2.2 keV at the 1.3 MeV ^{60}Co γ ray. Standard modular electronics have been used and data were accumulated and stored using the PDP-15 on line computer of the tandem accelerator laboratory.

In Fig. 1, a γ -ray spectrum of the $^{64}\text{Zn} + ^7\text{Li}$ reaction is displayed, collected at a bombarding energy of 18 MeV ^7Li and at a $\Theta_\gamma = 90^\circ$ with respect to the beam. The Q value for the $^{64}\text{Zn} + ^7\text{Li}$ reaction leading to ^{69}Ga is +980 keV and thus at the above mentioned bombarding energies we expect a substantial feeding of a large number of excited states with relatively high spin values in the ^{69}Ga residual nucleus. For the other exit channels which are energetically possible, we have observed ^{69}Zn and ^{68}Zn arising from the (p, n) and $(p, 2n)$ exit channels, ^{68}Ga from the $3n$ channel, and ^{65}Cu and ^{66}Cu from the (αn) and $(\alpha 2n)$ channels, respectively. (See Fig. 1.)

B. Coincidence experiments

The construction of the decay scheme of the ^{69}Ga residual nucleus was entirely based on the results of the coincidence experiment. For this experiment the two above mentioned detectors have been used,

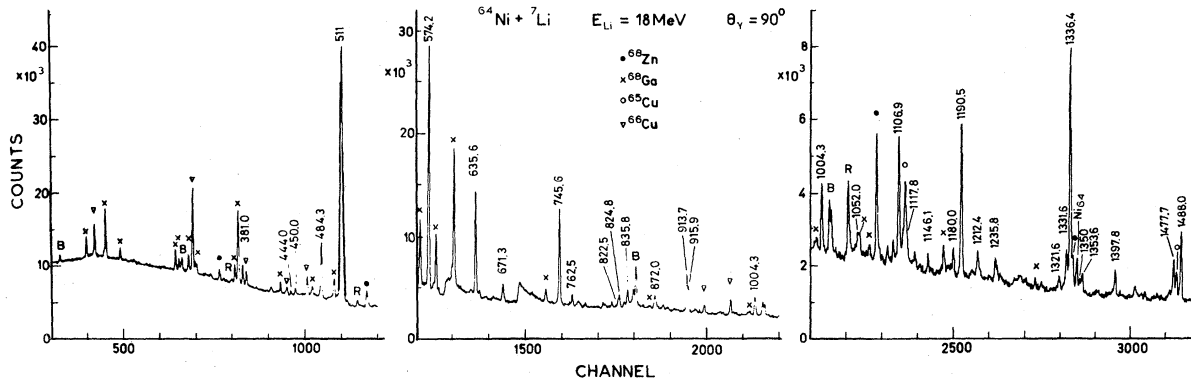


FIG. 1. Gamma ray spectrum of the $^{64}\text{Ni} + ^7\text{Li}$ reaction at 18 MeV ($\theta_\gamma = 90^\circ$).

being located at $+90^\circ$ and -90° with respect to the beam. Although the configurations where $\Theta_{\gamma_1} = 90^\circ$ and $\Theta_{\gamma_2} = 0^\circ$ in coincidence experiments yield valuable information on the studied γ -ray transitions in the framework of a directional correlation from oriented states (DCO) analysis, we have deliberately avoided this configuration because both detectors were already heavily exposed to neutrons and thus judged not suitable to maintain the high neutron flux at 0° for the long time period required in the coincidence experiments. Data accumulation was performed with the PDP-15 computer, by an event by event storage of the information. The data stored were the analog signals of the two Ge(Li) detectors and the time information from the time-to-amplitude converter (TAC). In the present experiment a total of 10^7 events have been recorded on magnetic tapes. The required coincidence spectra were constructed by a replay program when a time gate of about 25 ns was set on the prompt time spectrum. For each required gate a spectrum coincident with the gate was constructed as well as a background spectrum which was obtained by setting a gate of equal spacing on the γ -ray background at a suitable position on the right of each photopeak studied. In Figs. 2 and 3, some representative coincident spectra after background subtraction are shown. The decay scheme of ^{69}Ga resulting from the analysis of all the coincidence spectra is shown in Fig. 4.

C. Angular distributions

Angular distributions of emitted γ rays from the residual ^{69}Ga nucleus have been measured at 18 MeV bombarding energy. The 18% efficiency detector was mounted on an angular distribution

table with the face of the detector at a distance of 10 cm from the target. Data were collected at 0° , 15° , 30° , 55° , 70° , 90° , 110° , and 120° with respect to the beam axis. The 13% efficiency detector was located at -90° with respect to the beam and served as a monitor. The scattering chamber was a miniature aluminum cylindrical chamber lined internally with Ta foil. Alignment of the detector-scattering chamber assembly was checked via a radioactive point source, and subsequently on line, by using γ rays showing isotropic distribution (e.g., the 843 keV Al line as well as the 397 keV γ -ray deexciting the isomeric $\frac{9}{2}^+$ state in ^{69}Ge).

During these experiments, although low currents were used and the dead time was restricted to about 15%, a pulser was used which was fed to both detectors used in the experiments, in order to measure relative changes of the dead time rate. The experimental angular distributions were fitted by least squares procedures to a Legendre polynomial expansion

$$W(\vartheta) = \sum_{\nu=0}^4 Q_\nu A_\nu P_\nu(\cos\vartheta), \quad \nu = \text{even}, \quad (1)$$

where Q_ν are the appropriate solid angle correction factors of the detector. The measured angular distribution coefficients A_ν , besides the electromagnetic information, are also composed¹⁰ of the theoretical coefficient of maximum alignment B_ν^{max} times a spin alignment attenuation coefficient $\alpha_\nu(J_i)$

$$B_\nu(J_i) = \alpha_\nu(J_i) \cdot B_\nu^{\text{max}}(J_i). \quad (2)$$

The attenuation coefficients $\alpha_\nu(J_i)$ necessary to extract information from the presently measured angular distributions have been determined experimentally by measuring the angular distribution of several γ rays of well known multipolarity proceed-

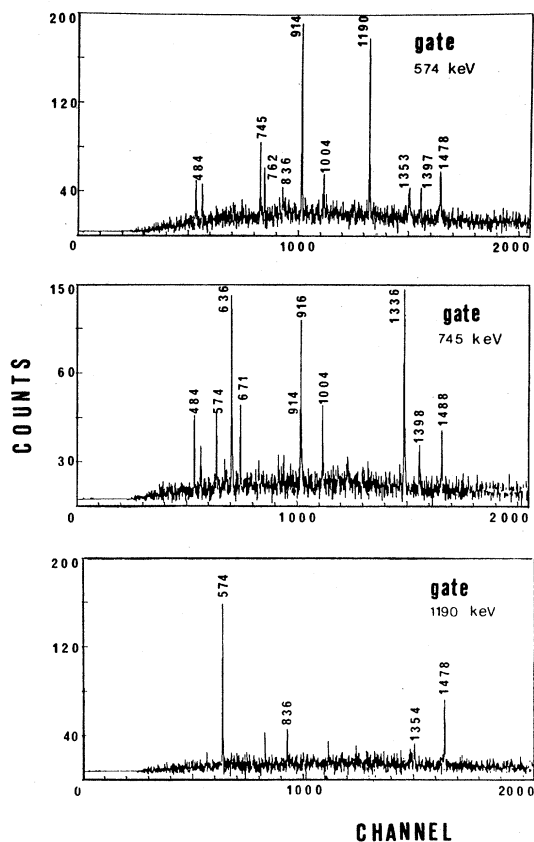


FIG. 2. Coincidences spectra obtained by gating with 574, 745, and 1190 keV γ rays.

ing between states of known spin in different nuclei. The nuclei chosen, the populating reactions, and the proper references⁷⁻¹⁸ are listed in Table I. The measured angular distribution and the known elec-

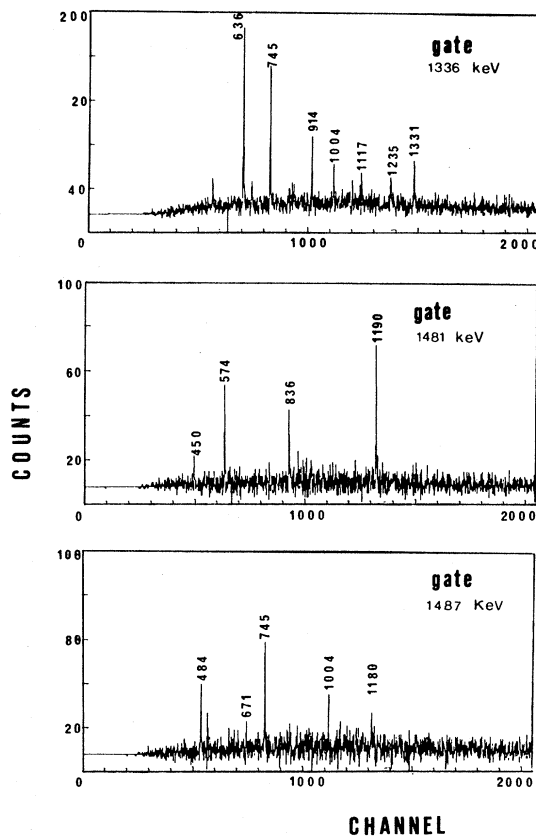


FIG. 3. Coincidences spectra obtained by gating with the 1336, 1481, and 1487 keV γ rays.

tromagnetic properties of the levels involved were used in Eqs. (1) and (2) to determine the appropriate $\alpha_n(J_i)$. Most of the levels chosen among the nuclei shown in Table I were mainly populated by side

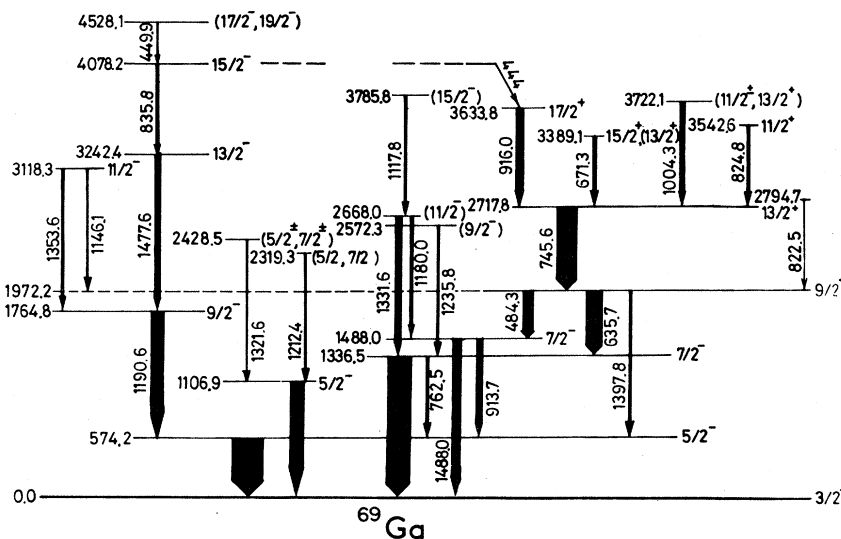


FIG. 4. The resulting decay scheme of ^{69}Ga .

TABLE I. List of nuclei, their corresponding reactions, and reference data used to estimate attenuation coefficients of the angular distributions. (All reactions are carried at $E_{Li} = 18$ MeV.)

Nucleus	Reaction	References
^{69}Ge	$^{64}\text{Zn} + ^7\text{Li} \rightarrow ^{69}\text{Ge} + pn$	11,12,13
^{69}Ga	$^{64}\text{Ni} + ^7\text{Li} \rightarrow ^{69}\text{Ga} + 2pn$	7,8,9
^{67}Ga	$^{62}\text{Ni} + ^7\text{Li} \rightarrow ^{67}\text{Cu} + 2n$	14,15
^{65}Ga	$^{60}\text{Ni} + ^7\text{Li} \rightarrow ^{65}\text{Ga} + 2n$	16
^{69}As	$^{64}\text{Zn} + ^7\text{Li} \rightarrow ^{69}\text{As} + 2n$	17
^{65}Cu	$^{64}\text{Ni} + ^7\text{Li} \rightarrow ^{65}\text{Cu} + a 2n$	18

feeding. For some of the levels, especially those of lower spin, substantial feeding is present by γ rays from higher lying states. In all such cases a correction for this feeding was applied and thus the derived $\alpha_v(J_i)$ represents attenuation arising from side feeding. All $\alpha_v(J_i)$ data obtained are shown in Fig. 5 as a function of J_i . At this point it is appropriate to remark that the experimentally measured $\alpha_v(J_i)$ cannot be reproduced by an assumption of a Gaussian distribution of the magnetic substates.

In contrast it has been found that an assumption of a simple exponential distribution of the magnetic substates of the form

$$p(m) = c \exp\{-m/2.2\} \quad (3)$$

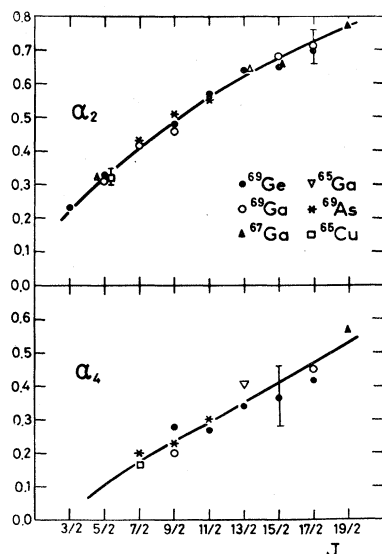


FIG. 5. Experimentally determined attenuation parameters as a function of spin. The solid line is a fit to the data using a simple exponential function (see text for discussion).

gave a nice agreement for both $\alpha_2(J_i)$ and $\alpha_4(J_i)$ in the experiment. The calculated $\alpha_v(J_i)$ values with the help of Eq. (3) are shown in the form of a curve in Fig. 5. The inadequacy of a Gaussian assumption for the magnetic substates distribution has also been noticed previously by other workers,^{19,20} although for some reactions it has been reported that Gaussian magnetic substates are compatible with experimental data.¹⁴ In applying Eqs. (1) and (2) in the present case, the alignment B_v of a particular level with spin J_i was calculated by taking the weighted mean

$$B_v(J_i) = \frac{1}{I_\gamma + I_s} [\alpha_v(J_i) \cdot B_v^{\max}(J_i) I_s + B_v(J_i') \cdot U(J_i' \rightarrow J_i) \cdot I_\gamma], \quad (4)$$

where $U(J_i' \rightarrow J_i)$ is the deorientation¹⁰ parameter of the cascading γ ray which originates from a higher level J_i' with intensity I_γ , while I_s is the side feeding intensity of the level J_i . Equation (4) can trivially be extended to accommodate more than one cascade γ ray.

D. Mean life measurements

The Doppler shift attenuation (DSA) technique has been used to determine mean lives of excited states. The centroid position of the γ rays as a function of the angle of observation has been determined for numerous transitions. The theoretical Doppler shift attenuation curves $F(\tau)$ have been calculated by using the Blaugrund²¹ formalism and assuming

$$T_t = f_e T_e + f_n T_n, \quad (5)$$

where T_t is the total stopping power and T_e and T_n are the electronic and nuclear stopping powers, respectively, as given by the Lindhard²² theory, while f_e and f_n are adjustable parameters.

The effect of the finite thickness of the target and the ions recoiling into the vacuum (about 6% of the totals) has been taken into account. By setting $f_e = f_n = 1$ the resulting curve gives a mean life for the 1346 keV $^{64}\text{Ni } 2_1^+$ state excited by the inelastic scattering of the Li ions of $\tau = (1.4 \pm 0.2)$ ps, in good agreement with the known mean life of this state. In evaluating the mean life of the levels in ^{69}Ga by unobserved transitions originating from the continuum has been taken into account by assuming $\tau_s = 0.1$ ps, a value which is commonly used in this mass region.¹³

III. RESULTS

The measured gamma ray energy, intensity, and angular distribution expansion coefficients for the ^{69}Ga transitions are shown in Table II. The yield ratio of the ^{69}Ga transitions at the two bombarding energies of 18 and 16 MeV are given in Table III and are used also to help spin assignments. The mean lives deduced for ^{69}Ga levels from the DSA experiments are given in Table IV.

For the lower lying levels of ^{69}Ga (Fig. 4), namely the 574, 1106.9, 1336.5, 1488, 1764.8, and 1972.2 keV levels, a general agreement concerning mixing ratios and mean lives is observed between the present and previously published data. For the 1764.8 keV, for which no previous mean life measurement is available, the present experiments (Table IV) yield a value of $\tau = 1.2 \pm 0.2$ ps.

For the higher lying levels the following remarks can be made:

(i) *The 2717.8 keV level.* This level deexcites by the 745.6 keV γ ray to the $\frac{9}{2}^+$ 1972.2 keV level. This level has been observed also by Harms-Ringdahl *et al.*⁹ These authors have assigned a $J^\pi = \frac{9}{2}^+$ to this level on the grounds of the yield ratio, although their measured angular distribution showed a χ^2 min compatible with both $\frac{9}{2}^+$ and $\frac{13}{2}^+$ spin and parity assignments. In a recent review of the $A=69$ chain, Auble⁵ considered the $\frac{9}{2}^+$ assignment to this level a tentative assignment. In contrast, our measured angular distribution of the strongly excited 745 keV γ ray (Table II) points to a unique $J^\pi = \frac{13}{2}^+$ spin and parity assignment to this level. The chi-square fit of the data (shown in Fig. 6) rejects the $\frac{9}{2}$ spin hypothesis at the 0.1% confidence limit. In addition, the yield of the 745 keV γ ray (Table III) increases much more rapidly than the corresponding yield of the γ rays deexciting the 1765 keV $\frac{9}{2}^-$ level (Table III), indicating a $J \geq \frac{11}{2}$. Thus a unique $J^\pi = \frac{13}{2}^+$ spin and parity is adopted for the 2717.8 keV level. The measured $F(\tau)$ for the 745 keV γ -ray yield a limit of $\tau \geq 2$ ps for the mean life of this level.

(ii) *The 3633.8 keV level.* This level has been established on the basis of the observed coincidences between the pair of 916 and 745 keV γ rays. The 916 keV γ ray forms a doublet with the 913.7 keV γ ray deexciting the 1488 keV level (see Fig. 1). This doublet has been analyzed in two ways: (a) by assuming a Gaussian distribution of the photopeak to separate the two components of the complex peak, and (b) by subtracting from each complex peak at

each angle, the contribution of the 913.7 keV γ ray, since for this peak both relative intensity with respect to the 1488 keV crossover transition as well as the mixing ratio of the 913.7 keV γ ray is known accurately.^{7,8} By applying both methods a consistent set of angular distribution coefficients for both γ rays has been obtained (Table III). The measured angular distribution of the 916 keV γ ray is consistent with a spin and parity assignment of $J^\pi = \frac{17}{2}^+$ or $\frac{13}{2}^+$ (see Fig. 6). The yield ratio of 3.1 for the 916 keV γ ray (Table III) indicates a spin of $J \geq \frac{17}{2}$. Thus we adopt a $\frac{17}{2}^+$ spin and parity for this level. The interference of the 913.7 keV γ ray is more severe in the case of estimating the centroid shift of the 916 keV. The present data give a tentative estimate of $\tau = 2 \pm 1$ ps for the mean life of this level.

(iii) *The 3389.1 keV level.* This level has been established on the basis of the observed coincidences between the pairs of 671 and 745 keV γ rays. The measured angular distribution of the 671/p keV γ ray (Fig. 6) is consistent with $J = \frac{11}{2}$, $\frac{13}{2}$, and $\frac{15}{2}$. The yield ratio (Table III) suggests $J = \frac{15}{2}$ and $\frac{17}{2}$. We thus adopt a tentative $J = \frac{15}{2}$ spin assignment but certainly the $\frac{13}{2}$ assignment cannot be ruled out. In both cases the resulting mixing ratio is large enough to exclude an $E1$ transition, and thus we limit the J^π values $\frac{15}{2}^+$ ($\frac{13}{2}$)⁺. The measured mean life of this state is $\tau = 2.7 \pm 1.5$ ps.

(iv) *The 3722.1 keV level.* This level has been established on the basis of the 1004-745 keV pair of coincidences. The measured angular distribution of the 1004 keV γ ray (Fig. 6) is consistent with $J = \frac{11}{2}$, $\frac{13}{2}$, and $\frac{15}{2}$. The yield ratio is consistent with $J = \frac{9}{2}$, $\frac{11}{2}$, or $\frac{13}{2}$. We thus adopt a $J = \frac{11}{2}$ or $\frac{13}{2}$ for this level. The measured mean life of 2.3 ± 0.4 ps and the resulting mixing ratios limit the spin and parities to $J^\pi = \frac{11}{2}^\pm$ or $\frac{13}{2}^+$ for this level.

(v) *The 3542.6 keV level.* This level is established on the basis of the 824-745 pair of coincidences. The angular distribution of the 824 keV γ ray (Fig. 7) indicates a $J = \frac{11}{2}$ or $\frac{15}{2}$. The yield ratio indicates a $J < \frac{13}{2}$ for this level. The measured mean life of this state (Table IV) $\tau = 0.6(1)$ ps and the resulting mixing ratio, limit the assignment to $J^\pi = \frac{11}{2}^+$ for this level.

(vi) *The 3242.4, 4078.2, and 4528.1 keV levels.* These levels have been established on the basis of the observed coincidences between pairs of transitions including the 1190 keV γ ray and the 1477, 836, and 450 keV γ rays deexciting these levels.

TABLE II. Measured angular distribution of γ rays in the reaction ${}^{64}\text{Ni}({}^7\text{Li}, 2n\gamma){}^{60}\text{Ga}$ at $E = 18$ MeV. The attenuation coefficients α_2, α_4 used to extract the mixing ratios are also shown.

Level (keV)	E_γ	I_γ	J_i	J_f	M	A_2	A_4	α_2	α_4	Present	δ	Others
574.22(5)	574.22(5)	156	$\frac{5}{2}^-$	$\frac{3}{2}^-$	M1/E2	-0.189(10)	0.00(1)	0.37	0.11	-0.06(1)		-0.06(3) ^a
1106.94(5)	1106.94(5)	58	$\frac{5}{2}^-$	$\frac{3}{2}^-$	M1/E2	0.088(28)	0.01(4)	0.32	0.09	0.33(5)		0.41(5) ^a , 0.34(4) ^b , 0.32(2) ^c
1336.48(5)	1336.44(5)	125	$\frac{7}{2}^-$	$\frac{3}{2}^-$	E2	0.236(21)	-0.050(26)	0.48	0.14	0.00(2)		
	762.48(2)	9	$\frac{7}{2}^-$	$\frac{5}{2}^-$	M1/E2	0.49(9)	0.00(11)			-0.42 ^{+0.16} _{-0.40}		
										or		
1487.95(3)	1487.98(4)	43	$\frac{7}{2}^-$	$\frac{3}{2}^-$	E2	0.25(3)	-0.07(3)	0.49	0.17	-1.5 \pm 0.5		-2.0(4) ^b , -2.2(2) ^c
	913.71(5)	30	$\frac{7}{2}^-$	$\frac{5}{2}^-$	M1/E2	-0.36(3)	+0.13(4)			-2.3(2)		
	381.00(6)	14	$\frac{7}{2}^-$	$\frac{5}{2}^-$	M1/E2	-0.19(5)	0.03(5)			-0.01(6)		-0.03(3) ^c
1764.75(6)	1190.55(3)	70	$\frac{9}{2}^-$	$\frac{5}{2}^-$	E2	0.232(20)	0.062(25)	0.52	0.24	-0.02(3)		-2.54(10) ^a , -3.5(5) ^b , -2.85(30) ^c
1972.19(7)	635.68(3)	71	$\frac{9}{2}^+$	$\frac{7}{2}^-$	E1	-0.20(1)	0.00(2)	0.55	0.23	-0.01(2)		-0.03(3) ^c
	484.33(4)	49	$\frac{9}{2}^+$	$\frac{7}{2}^-$	E1	-0.19(1)	0.00(3)			0.00(2)		-0.03(3) ^c
	1397.81(15)	13	$\frac{9}{2}^+$	$\frac{5}{2}^-$	M2	0.22(9)	0.02(11)			-0.06(12)		
2319.31(15)	1212.37(10)	11	$\frac{7}{2}^-$	$\frac{5}{2}^-$	(E1 or M1)	-0.09(6)	0.07(8)	0.41	0.18	0.07(7)		
										or		
			$\frac{5}{2}^-$	$\frac{5}{2}^-$	M1/E2			0.32	0.13	-0.7(3)		
2428.58(25)	1321.64(20)	8	$\frac{7}{2}^-$	$\frac{5}{2}^-$	(M1/E2)	0.14(9)	-0.03(11)	0.41	0.18	0.35(20)		
										or		
			$\frac{5}{2}^-$	$\frac{5}{2}^-$	(E1 or M1)			0.32	0.13	0.0(2)		
2572.32(25)	1235.84(20)	8	$\frac{5}{2}^-$	$\frac{7}{2}^-$	M1/E2	-0.27(6)	0.05(7)	0.32	0.12	0.60(25)		
										or		
			$\frac{9}{2}^-$	$\frac{7}{2}^-$	M1/E2			0.49	0.23	-0.50(15)		
2668.07(10)	1331.63(6)	24	$\frac{11}{2}^-$	$\frac{7}{2}^-$	E2	0.23(5)	-0.06(6)	0.56	0.29	-0.03(6)		
										or		
			$\frac{9}{2}^-$	$\frac{7}{2}^-$	M1/E2			0.49	0.23	0.43(8)		
	1180.04(10)	11	$\frac{11}{2}^-$	$\frac{7}{2}^-$	E2	0.34(7)	-0.01(9)			0.13(14)		

TABLE II. (Continued.)

Level (keV)	E_γ	I_γ	$J_i J_f$	M	A_2	A_4	α_2	α_4	Present	δ	
										Others	Others
2717.80(9)	745.61(2)	100	$\frac{9}{2}^- - \frac{7}{2}^-$ or $\frac{13}{2}^+ + \frac{9}{2}^+$	M1/E2 E2	0.296(19)	-0.100(25)	0.61	0.32	0.62(12) -0.01(3)		
2794.70(50)	822.50(50)	5	$(\frac{7}{2}^+, \frac{9}{2}^+)$	M1/E2	0.17(7)	-0.04(8)	0.56	0.29	0.31(17)		
3118.30(20)	1353.55(20)	10	$\frac{11}{2}^- - \frac{9}{2}^-$ or $\frac{11}{2}^- - \frac{9}{2}^+$	E1	-0.16(11)	0.08(13)			0.02(11)		
3242.40(12)	1477.65(6)	26	$\frac{13}{2}^- - \frac{9}{2}^-$ or $\frac{13}{2}^- - \frac{9}{2}^+$	E2	0.32(3)	-0.11(4)	0.64	0.34	0.01(5)		
3389.15(12)	671.34(8)	17	$(\frac{15}{2}^+, \frac{13}{2}^+)$	M1/E2	0.38(3)	0.03(4)	0.68	0.41	0.50(4)		
3542.57(12)	824.77(8)	11	$\frac{11}{2}^+ + \frac{13}{2}^+$	M1/E2	0.42(2)	0.01(10)	0.56	0.29	0.35(15)		
3633.75(11)	1915.95(5)	31	$\frac{17}{2}^+ + \frac{13}{2}^+$ or $\frac{11}{2}^- + \frac{13}{2}^-$	E2	0.29(2)	-0.08(2)	0.72	0.47	0.00(2)		
3722.10(11)	1004.30(6)	25		(E1 or M1)	-0.11(3)	-0.03(4)	0.56	0.29	0.00(4)		
			or $\frac{13}{2}^+ + \frac{13}{2}^+$ or J_{-}^{15+}	M1/E2			0.62	0.35	-1.0(2)		
3785.85(15)	1117.78(10)	16	$(\frac{15}{2}^-) - (\frac{11}{2}^-)$	(E2)	0.22(4)	-0.11(5)	0.68	0.41			
4078.16(14)	835.76(7)	26	$\frac{15}{2}^- - \frac{13}{2}^-$	M1/E2	0.39(3)	-0.02(5)	0.68	0.41	0.52(7)		
	444.0(4)	4	$\frac{15}{2}^- - \frac{17}{2}^+$	(E1)	-0.12(13)	0.04(15)			$\delta \sim 0$		
4528.06(18)	449.90(10)	7	$\frac{19}{2}^- - \frac{15}{2}^-$ or $\frac{17}{2}^- - \frac{15}{2}^-$	(E2)	0.28(7)	0.01(10)	0.77	0.53	-0.04(8)		
				M1/E2			0.72	0.47	0.37(8)		

^aReference 6.^bReference 7.^cReference 8.^dReference 4.^eReference 9.

TABLE III. The ^{69}Ga γ -ray yield ratio R at 18 MeV relative to 16 MeV bombarding energy.

Level (keV)	γ ray (keV)	$R = Y(18)/Y(16)$	Known J^π	Proposed J
574	574	1.45(6)	$\frac{5}{2}^-$	
1336.5	1336.5	1.40(10)	$\frac{7}{2}^-$	
1488	1488	1.56(7)	$\frac{7}{2}^-$	
1764.8	1190.6	1.50(10)	$\frac{9}{2}^-$	
1972	635	1.72(7)	$\frac{9}{2}^+$	
	484			
2319	1212	1.40(20)		$\leq \frac{9}{2}$
2429	1321	1.50(15)		$\leq \frac{11}{2}$
2572	1235	1.50(20)		$\leq \frac{11}{2}$
2668	1331	1.50(10)		$\leq \frac{11}{2}$
	1180			
2717	745	2.02(10)	$\frac{13}{2}^+$	
3118	1353	1.65(10)		$\frac{11}{2}, \frac{9}{2}, \frac{7}{2}$
	1141			
3242	1478	1.90(10)		$\frac{13}{2}, \frac{11}{2}$
3542	825	1.75(15)		$\frac{13}{2}, \frac{11}{2}, (\frac{9}{2})$
3389	672	2.40(15)		$\frac{15}{2} (\frac{17}{2})$
3633	916	3.10(30)		$\frac{17}{2} (\frac{19}{2})$
3722	1004	1.85(15)		$\frac{13}{2}, \frac{11}{2}, (\frac{9}{2})$
3786	1118	2.3 (5)		$\frac{13}{2}, \frac{15}{2}, \frac{17}{2}$
4078	836	2.6 (25)		$\frac{15}{2}, (\frac{17}{2})$
4528	450	3.70(65)		$\geq \frac{17}{2}$

Their relative positions have been established on the basis of the observed intensities of the γ rays at 14, 16, and 18 MeV bombarding energies. The measured angular distribution of the 1477 γ ray (Fig. 7) indicates a $J = \frac{13}{2}^-$ or $\frac{9}{2}$ for the 3242 keV level, while the yield ratio indicates a $J = \frac{11}{2}$ or $\frac{13}{2}$. Thus a $J^\pi = \frac{13}{2}^-$ is adopted for this level for which a mean life of $\tau = 0.8$ ps is deduced (Table IV). The angular distribution of the 836 keV γ ray which deexcites the 4078 keV level (Fig. 7) is consistent with $J = \frac{11}{2}, \frac{13}{2},$ or $\frac{15}{2}$, while the yield ratio favors a $J = \frac{15}{2}$ or $\frac{17}{2}$. We thus adopt a $J = \frac{15}{2}^-$ for this level since the resulting mixing ratio and the measured mean life of $\tau = 0.8$ ps (Table IV) do allow the rejection of the positive parity. A weak γ ray of 444 keV observed to decay from this level to the 3633.8 keV $\frac{17}{2}^+$ shows an angular distribution consistent

with an $E1$ character, thus giving more strong support to the $J^\pi = \frac{15}{2}^-$ assignment to this level.

Finally, the 4528 keV level which deexcites by the 450 keV γ ray, shows an angular distribution (see Fig. 7) which is consistent with any spin assignment from $J^\pi = \frac{11}{2}$ up to $\frac{19}{2}$. The yield ratio for this γ ray indicates a spin of $J^\pi > \frac{17}{2}$. We tentatively assign a $\frac{17}{2}^-$ or $\frac{19}{2}^-$ for the spin and parity of this level to conform with the yield ratio of the deduced mixing ratios and mean life range of this level which is larger than 4 ps and less than 25 ns (the 450 keV is observed in the coincidence spectra).

(vii) *The other levels.* Based on the γ - γ coincidences new levels have been introduced at 2319.3, 2428.5, 2572.3, 2668.0, 2794.7, 3118.3, and 3785.8 keV. The measured angular distributions have been used along with the yield ratio to assign possible J values. The results for these levels are given in Table II, while the measured mean lives of these states are given in Table IV. The χ^2 fits to the angular distributions of the γ rays deexciting some of these levels are given in Fig. 8.

IV. DISCUSSION

The level structure of ^{69}Ga (Fig. 4) revealed by the present investigation indicates the presence of at least two distinct bands, one of a positive parity, based on a $\frac{9}{2}^+$ level, and another of a negative parity, based on a $\frac{9}{2}^-$ state. The ^{67}Ga nucleus studied by Zobel *et al.*¹⁴ shows a richness of positive parity high spin states, but no firm indication exists for a

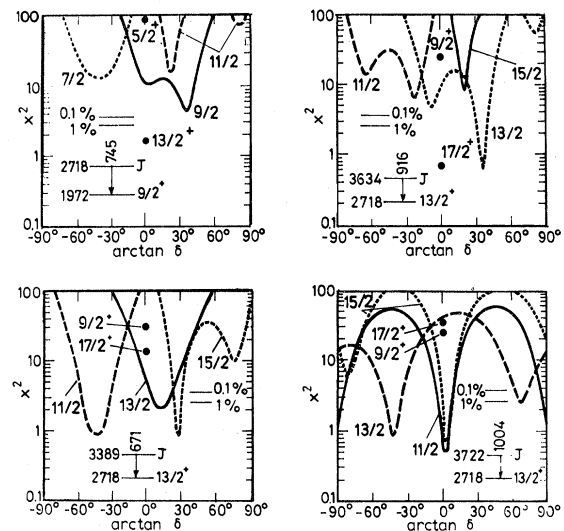


FIG. 6. The χ^2 fit to the measured angular distribution for the 745, 916, 671, and 1004 keV γ rays.

TABLE IV. Mean lifetime for ⁶⁹Ga levels, obtained by the DSAM centroid shift measurement in singles spectra obtained at bombarding energy of 18 MeV.

Level (keV)	γ ray used (keV)	F(τ)	τ (ps) Present	Others
1106.9	1106.9	0.147(7)	0.32(4) ^a	0.32(3) ^c
1336.5	1336.5	0.043(3)	1.5 ^{+0.2a} _{-0.5}	1.3 (3) ^c
1488.0	1488.0	≤ 0.04	≥ 2.5 ^a	6 ± 2 ^d
1764.8	1190.6	0.090(5)	1.2 (2) ^a	
1972.2	635.7	0.05	≥ 4	
2319.3	1212.4	0.09(2)	1.5 (3)	≥ 0.3 ^e
2428.5	1321.6	0.08(3)	≥ 2.5(1.1)	
2668.0	1331.6, 1180	0.045(8)	≥ 2.5 ^a	
2717.8	745	0.051(4)	≥ 2 ^a	
3118.3	1353.6, 1161.1	0.26(4)	0.34(7)	
3242.4	1477.6	0.06(1)	0.7 (4) ^a	
		0.14(2) ^b	0.80(15)	
3389.1	671.3	0.07(2)	2.7 (15)	
3542.6	824.8	0.17(2)	0.60(10)	
3633.8	916	0.09(3) ^a	2 ± 1	
3722.1	1004.3	0.07(1)	2.3 (4)	
3785.8	1117.8	0.09(2)	1.5 (3)	
4078.2	835.8	0.10(1)	0.80(15) ^a	
4528.1	450	≤ 0.05	≥ 4	

^aCorrected for feeding from above.

^bValue obtained at 16 MeV.

^cReference 6.

^dReference 3.

^eReference 8.

negative parity band analogous to the one observed here. Unlike ⁶⁷Ga, the ⁶⁵Ga nucleus studied by Kawakami *et al.*¹⁶ shows a striking similarity with ⁶⁹Ga, exhibiting both positive and negative parity

bands.

From the measured mean lives, we can conclude that most of the levels observed to deexcite by *E*2 transitions bears a significant collectivity. For ex-

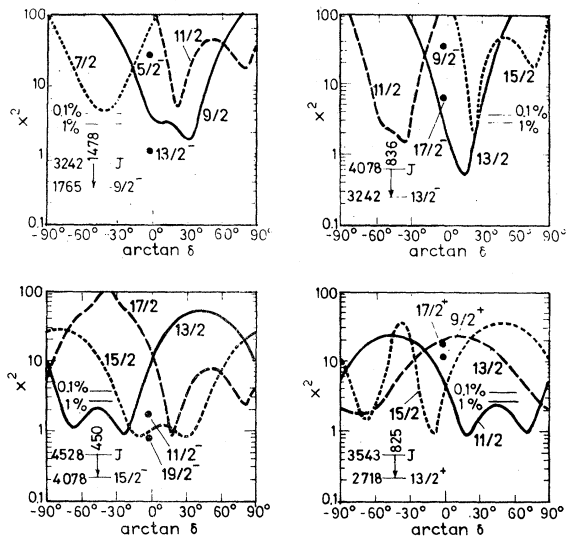


FIG. 7. The χ^2 fit to the measured angular distribution for the 1478, 836, 450, and 825 keV γ rays.

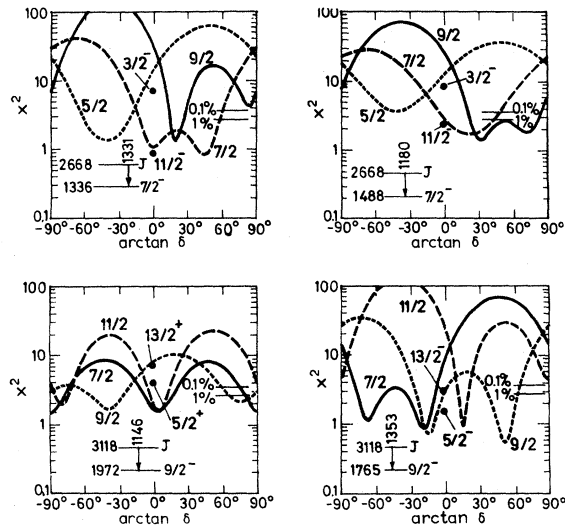


FIG. 8. The χ^2 fit to the measured angular distribution for the 1331, 1180, 1146, and 1353 keV γ rays.

ample, the $\frac{13}{2}^- \rightarrow \frac{9}{2}^- \rightarrow \frac{5}{2}^-$ sequence deexcites by two $E2$ transitions with a strength of about 10 W.u., and the situation in ^{65}Ga looks¹⁶ similar. For the transitions deexciting the positive parity band the upper limits of the mean lives measured here do not allow a reliable estimate of the strength of the $E2$ transitions.

Although the gross structure of ^{69}Ga may be interpreted in terms of particle-core coupling of the form $\{g_{9/2} \times J\}_{I^+}$ and $\{f_{5/2} \times J\}_{I^-}$ with $J=0^+$, 2^+ , 4^+ , 6^+ , the energy separation between successive multiplets becomes shorter with increasing J ,

indicating a more complex structure and probably a further core polarization by the extra proton. Another possible description of the nucleus may be given in the framework of a triaxial model as discussed in the case of ^{65}Ga by Kawakami.¹⁶ At this point, what seems more important in order to understand the high spin structure of the odd gallium isotopes is the need for additional experimental information in ^{65}Ga and ^{69}Ga , and especially mean life measurements in the range of 2 to 10 ps, the region in which we expect to find the mean life of the levels belonging to the positive parity band.

-
- ¹W. H. Zoller, C. E. Gordon, and W. B. Walters, Nucl. Phys. **A124**, 15 (1969).
- ²D. E. Velkley, K. C. Chung, A. Mittler, J. D. Brandenberger, and M. T. McEllistrem, Phys. Rev. **179**, 1090 (1969).
- ³R. G. Arnold, E. C. Booth, and J. W. J. Alstron, Phys. Rev. C **7**, 1490 (1973).
- ⁴T. Paradellis, A. Xenoulis, and C. A. Kalfas, Z. Phys. A **275**, 269 (1975).
- ⁵R. L. Auble, Nucl. Data Sheets **17**, 193 (1976).
- ⁶T. Paradellis and G. Vourvopoulos, Phys. Rev. C **18**, 660 (1978).
- ⁷D. Kaipov, Y. Kosyak, S. Arymov, and I. Shukalev, Yad. Fiz. **30**, 1198 (1979) [Sov. J. Nucl. Phys. **30**, 623 (1979)].
- ⁸T. Paradellis, G. Vourvopoulos, G. Costa, and E. Sheldon, Phys. Rev. C **24**, 398 (1981).
- ⁹L. Harms-Ringdahl, J. Sztarkier, and Z. P. Sawa, Phys. Scr. **2**, 15 (1974).
- ¹⁰T. Yamazaki, Nucl. Data Tables **A1**, 453 (1966).
- ¹¹Y. Zobel, L. Cleeman, J. Eberth, W. Neumann, and N. Wiehl, Phys. Rev. C **12**, 811 (1979).
- ¹²T. Paradellis, G. Costa, R. Seltz, C. Lebrun, D. Ardouin, F. Guilbault, M. Vergnes, and G. Berrier, Nucl. Phys. **A330**, 216 (1979).
- ¹³T. Paradellis and C. A. Kalfas, Phys. Rev. C **25**, 350 (1982).
- ¹⁴V. Zobel, L. Cleeman, J. Eberth, W. Neumann, and N. Wiehl, Nucl. Phys. **A316**, 165 (1979).
- ¹⁵A. M. Al. Naser, A. H. Behbehani, L. L. Green, A. N. James, C. J. Lister, P. J. Nolan, N. Rammo, J. F. Sharpey-Schafer, L. Zybert, and R. Zybert, J. Phys. G **4**, 1611 (1978).
- ¹⁶H. Kawakami, A. P. de Lima, R. M. Ronningen, A. V. Ramayya, J. H. Hamilton, R. L. Robinson, H. J. Kim, and L. K. Peker, Phys. Rev. C **21**, 1311 (1980).
- ¹⁷H. P. Heillmeister, E. Schmidt, M. Uhrmacher, and R. Rascher, Phys. Rev. C **17**, 2113 (1978).
- ¹⁸R. L. Auble, Nucl. Data Sheets **16**, 351 (1975).
- ¹⁹G. A. P. Engelbertink, L. P. Ekstrom, D. E. Scherpenzeel, and H. H. Eggenhusen, Nucl. Instrum. Methods **143**, 161 (1977).
- ²⁰L. P. Ekstrom, A. M. Al-Naser, P. L. G. Lornie, and P. J. Twin, Nucl. Instrum. Methods **158**, 243 (1979).
- ²¹A. E. Blaugrund, Nucl. Phys. **88**, 502 (1966).
- ²²L. Lindhard, M. Scharff, and H. E. Shjøtt, K. Dan. Vidensk. Selsk., Mat. Fys. Medd. **33**, No. 14 (1963).